ELSEVIER

Physica C 277 (1997) 257–264

PHYSICA C

Local structure anomalies of the $BaBi(Pb)O_3$ system at low temperatures: an X-ray absorption study

A.P. Menushenkov [a,*], S. Benazeth [b], J. Purans [c], A.Yu. Ignatov [a], K.V. Klementev [a]

[a] *Moscow Engineering Physics Institute, 115409 Moscow, Russia*

[b] *Laboratoire pour l'Utilisation du Rayonnement Électromagnétique 91405-Orsay and Laboratoire de Chimie Inorganique, Universite Paris Sud, 92296 Centre de Chatenay-Malabry, France*

[c] *Institute of Solid State Physics, Latvia University, 226063 Riga, Latvia*

Received 8 April 1995; revised manuscript received 9 December 1996

Abstract

Temperature dependent X-ray absorption investigations were made on the Bi L_3 edge in $BaPb_{1-x}Bi_xO_3$ with $x = 0.0$, 0.75 and 1.0. Essential local structure anomalies around Bi atoms were observed in $BaBiO_3$ and $BaPb_{0.25}Bi_{0.75}O_3$ at low temperatures. It is found that Bi–O, Bi–Ba distances abnormally increase with the temperature decreasing from 90 K. These anomalies are accompanied by an abnormal behaviour of the Debye–Waller factor σ^2 of the Bi–O bonds at low temperatures in contrary to the Einstein model. The lengths and σ^2 of the Pb–O and Pb–Ba bonds of $BaPbO_3$ show an ordinary increase with temperature. The anomalies are shown to be due to the rotation distortion asymmetry of the oxygen octahedra owing to the difference in the strength of Bi–O bonds. The experimental results are discussed in the frame of the dynamic fluctuation rotation mode.

Keywords: EXAFS; BPB; Thermal fluctuation; Low temperature

1. Introduction

An important question in understanding of HTSC phenomena is whether equivalent pairing mechanisms are applied to both copper and bismuth oxides. Superconductivity in the $BaPb_{1-x}Bi_xO_3$ (BPB) was discovered considerably earlier [1] than in cuprates [2]. However, there is no generally accepted description of the mechanism of superconductivity in these alloys so far. Moreover, it is not clear if the paring mechanism is the same in the similar compounds of BPB and $Ba_{1-x}K_xBiO_3$ (BKB) [3].

The phase diagram and the temperature dependent structure were the subject of considerable controversy for superconducting BPB alloys ($0 < x < 0.35$) and for both BPB end members: $BaBiO_3$ and $BaPbO_3$ (e.g. [4]). In the diffraction studies [5–8] an essential anisotropy in the thermal vibration of oxygen atoms for both BPB and BKB systems was found and it was shown that anisotropic thermal parameters of the bridging oxygen atoms are oblate along the Bi–O–Bi bonds which indicates a rocking motion or a possible disorder involving a tilting of the oxygen octahedra

* Corresponding author. Tel.: (7) 95 3239020; fax: (7) 95 3242111; e-mail: menushen@htsc.mephi.ru

PII S0921-4534(97)00083-X

[4]. Along with the structure uncertainties Heald et al. [9] observed some peculiarities of the Ba(K)BiO local structure at low temperatures using X-ray absorption spectroscopy. Two different temperature dependencies of the Debye–Waller factor σ^2 were found for two Bi–O bonds in $BaBiO_3$. For the superconducting material ($Ba_{0.6}K_{0.4}BiO_3$) the σ^2 temperature behaviour showed a significant deviation from the Einstein model. In addition, an abnormal increase of both the Bi–O distances with the temperature decrease was obtained for a pure and slightly potassium doped $BaBiO_3$ by Salem-Sugui et al. [10].

All these uncertainties seem to arise from the complexity of the BaPbBiO and BaKBiO structures due to two unequal Bi positions. To clarify these uncertainties, more rigorous studies of both the structural and local distortions and their temperature dependencies must be done.

In this paper an EXAFS-study of the local structure anomalies for the BaPb(Bi)O compounds which are more pronounced at low temperatures is presented and their nature is discussed in the frame of perovskite structure peculiarities.

2. Experiment

The samples of composition with $x = 0$, 0.75 and 1.0 were prepared by heating mixtures of oxides and carbonates ($BaCO_3$, Pb_3O_4 and Bi_2O_3) in air at 800–1000°C. The powder samples were annealed three times, subsequently ground and then slowly cooled. All the samples had a pure phase, which was examined by X-ray diffraction. For the XAFS measurements the fine powder was sedimented on micropore substrates. Their thickness was about 2 absorption lengths at the Bi(Pb) L_3 edge.

The X-ray absorption measurements were performed on D21 beam line of the DCI storage ring at Laboratoire pour l'Utilisation du Rayonnement Électromagnétique (LURE, Orsay, France), using a Si(111) double-crystal monochromator. The storage ring was operated at 1.85 GeV positron beam energy and 300 mA maximum current. The energy resolution was ~ 3 eV at 13 keV. The low temperature measurements were carried out with a liquid helium circulation cryostat. The temperature was regulated by a helium flow and measured with a carbon probe with the accuracy of 1 K.

3. EXAFS data reduction

First, the slowly varying background absorption was subtracted by extrapolation of the pre-edge part of the spectra. The XAFS function was determined as $\chi(E) = [\mu(E) - \mu_0(E)]/\mu_0(E)$, where $\mu(E)$ is the absorption cross section, $\mu_0(E)$ is the free atomic absorptance, which was approximated by a series of cubic splines. Finally, the data were transformed to k-space according to $k = [2m_e/\hbar^2(E - E_0)]^{1/2}$, where E_0 is the energy at the maximum of the first derivative of $\mu(E)$. The resulting XAFS function

$$\chi(k) = \sum_j \left\{ N_j F_j(k) \sin\left[2kR_j + \varphi_j(k)\right] \times \exp\left(-2k^2\sigma_j^2 - 2R_j/\lambda_j(k)\right)\right\}/kR_j^2$$

contains information about the near neighbour distances R_j, the Debye–Waller-type broadening σ_j^2, and the number of neighbours N_j in j shell around the absorber. The phase shift $\varphi_j(k)$ (depending on both the absorber and the scatterer), the scattering amplitude $F_j(k)$ and the electron free path $\lambda(k)$ were calculated using the FEFF-5 code.

The XAFS function $\chi(k)$ was Fourier transformed (FT) to real space with as long k-interval as possible. Separate peaks seen in the absolute value of the transform contain the structural information about the shell of interest. Using the back FT with a corresponding windowing function, $\chi(k)$ related to a single sphere was obtained. To get values of R_j, σ_j^2, and N_j, we performed least-squares non-linear fit to the single spheres obtained.

The closeness of L_3 Pb (13.035 keV) and Bi (14.418 keV) edges complicates the quantitative analysis of the mixed compounds ($x \neq 0$, 1.0). The Pb background is noticeably above the Bi L_3 edge and should be subtracted. A way of solving this problem is to construct a model using the data between the Pb and Bi L_3 edges [11] and to prolong it over the Bi L_3 edge. Here the subtraction of the $\chi(k)$ of the $BaPbO_3$ experimental spectra (Pb L_3 edge) taken at the same temperature was used. In this case the subtracted spectrum contained information

about all the coordination shells (in contrary to the subtraction of the model $\chi(k)$ that contains only 2 or 3 shells). At the same time there is some difference between the local environment of Pb in the mixed compounds and in $BaPbO_3$, and for the $x = 0.75$ compound this difference is not negligible. Nevertheless, the Pb absorptance is three times as small as the absorptance of Bi and some shortage of accuracy in such a small Pb background is less important.

4. General results

4.1. Pb, Bi edges

For $BaPbO_3$ ($x = 0$) and $BaBiO_3$ ($x = 1$), the XAFS data were obtained by the Fourier transform (FT) (see Fig. 1) over the range $3. \div 14$ Å^{-1} in k-space. The back Fourier transform (BFT) was provided using square windows $1.0 \div 2.1$ Å for Pb–O and Bi–O shells and $2.5 \div 4.0$ Å for the Pb(Bi)–Ba shell (see Fig. 2).

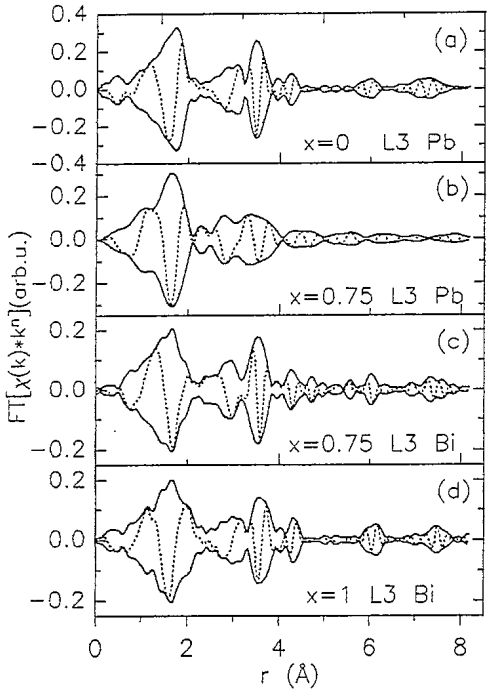

Fig. 1. EXAFS in r space (Fourier transform): (a) Pb L_3 edge for $BaPbO_3$; (b) Pb L_3 edge for $BaBi_{0.75}Pb_{0.25}O_3$; (c) Bi L_3 edge for $BaBi_{0.75}Pb_{0.25}O_3$; (d) Bi L_3 edge for $BaBiO_3$.

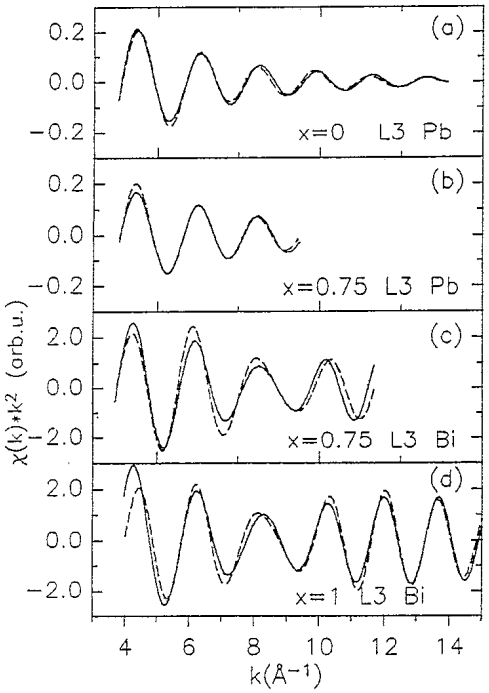

Fig. 2. Examples of fits of oxygen shell for $BaBi_xPb_{1-x}O_3$: (a) Pb L_3 edge for $BaPbO_3$; (b) Pb L_3 edge for $BaBi_{0.75}Pb_{0.25}O_3$; (c) Bi L_3 edge for $BaBi_{0.75}Pb_{0.25}O_3$; (d) Bi L_3 edge for $BaBiO_3$.

For the $x = 0.75$ compound, FT k-range on Pb L_3 edge is limited by 9.6 Å^{-1}, where the Bi L_3 edge begins. This broadens the peaks of the FT and, hence, produces some uncertainties in the amplitudes and the Debye–Waller factors extracted from the Pb part of the spectra.

Data from the Bi L_3 fine structure were extracted after the subtraction of the oscillating background from Pb L_3 edge. For this procedure we used the Pb L_3 XAFS from $BaPbO_3$ measured at the same temperatures. The Pb L_3 XAFS was transformed back to the energy scale ($E = E_0 + \hbar^2 k^2 / 2m_e$) and renormalised to the step height at the Pb L_3 edge: $\mu(E) = \chi(E)\mu_0(E) + \mu_0(E)$. This spectrum completely reproduces the area between Pb L_3 and Bi L_3. After subtraction the EXAFS spectrum that is relatively free of the Pb L_3 edge contribution was obtained. Then, using the forward and back FT, the partial spheres of the oxygen and barium for all the compounds were acquired (see Fig. 2).

4.2. Detailed comparison

To get numerical results a non-linear least-squares fit in the k-space was performed. The Pb(Bi)–O and Pb(Bi)–Ba distances are summarised in Table 1 with an error of ~ 0.01 Å.

For the Pb first neighbour environment there is only one Pb–O distance for both $x = 0$ and $x = 0.75$ compounds. The thermal expansion caused an ordinary increase of the Pb–O and Pb–Ba distances as well as an increase of the Pb–O bond DW-factor (see Table 1).

For undoped $BaBiO_3$ (see Table 1) we have determined two Bi–O distances separated by 0.15 Å at 300 K and by 0.18 Å at 7 K. The difference between the two Bi–O bond lengths agrees with other XAFS studies and data of neutron diffraction: Boyce et al. [11] obtained 0.18 Å (80 K), Salem-Sugui et al. [10] 0.17–0.18 Å (5 ÷ 295 K), Thornton and Jacobson [12] 0.12 Å (300 K) and Chaillout et al. [13] 0.12 Å (300 K). The similar Bi–O distances were determined for the $x = 0.75$ compound: 0.13 (300 K) ÷ 0.15 Å (7 K). The amplitudes of the Bi(1)–O and Bi(2)–O partial contributions to the XAFS were considered to be equal.

4.3. Low temperature anomalies of the local structure

As was shown above, the mean Bi–O and the Bi–Ba distances for both $x = 1.0$ and $x = 0.75$ as well as Pb–Ba distance for $x = 0.75$ appear to contract with the temperature growth from 7 K to 90 K. The Bi–O distances contraction in $BaBiO_3$ was pointed out by Salem-Sugui et al. [10]. The abnormal contraction of Bi(Pb)–Ba distances with temperature growth is in a good agreement with the negative linear thermal coefficient of expansion found by Anshukova et al. [14] for a slightly doped BKB system at low temperature. At the same time Pei et al. [7] did not find any increase of $BaBiO_3$ lattice parameters at low temperature by the neutron diffraction.

Table 1
Results of EXAFS analysis

	T (K)	r(Pb–O) (Å)	σ^2 (10^{-3}Å^2)	r(Pb–Ba) (Å)	σ^2 (10^{-3}Å^2)		
$BaPbO_3$							
	7	2.15	0.76	3.76	3.1		
	30	2.16	0.93	3.76	3.5		
	80	2.16	1.04	3.76	3.9		
	90	2.17	1.20	3.76	3.9		
	100	2.17	1.42	3.77	4.0		
	250	2.18	1.44	3.77	8.1		
	T (K)	r(Bi–O)$_{1/2}$ (Å)	$\sigma^2_{1/2}$ (10^{-3}Å^2)	Δr (Å)	$\langle r\rangle$(Bi–O) (Å)	r(Bi–Ba) (Å)	σ^2 (10^{-3}Å^2)
$BaBiO_3$							
	7	2.34, 2.15	4.8, 2.3	0.19	2.24	3.83	2.9
	30	2.32, 2.14	4.3, 2.0	0.18	2.23	3.82	3.1
	55	2.31, 2.13	2.0, 0.7	0.18	2.22	3.81	3.7
	90	2.30, 2.14	2.4, 0.6	0.16	2.22	3.81	3.9
	250	2.29, 2.14	6.0, 3.0	0.15	2.22	3.80	7.0
	T (K)	r(Bi–O)$_{1/2}$ (Å)	Δr (Å)	$\langle r\rangle$(Bi–O) (Å)	r(Pb–O) (Å)	r(Bi–Ba) (Å)	r(Pb–Ba) (Å)
$BaPb_{0.25}Bi_{0.75}O_3$							
	7	2.29, 2.14	0.15	2.21	2.21	3.81	3.80
	30	2.28, 2.13	0.15	2.21	2.19	3.81	3.79
	55	2.26, 2.12	0.14	2.19	2.19	3.80	3.78
	250	2.25, 2.12	0.13	2.18	2.18	3.79	3.77

With decreasing temperature, the difference between two Bi–O bond lengths appears to increase from 0.15 Å (300 K) to 0.18 Å (7 K) due to the increase of the longer Bi–O bond length [2.29 Å (300 K) ÷ 2.34 Å (7 K)]. At the same time the shorter Bi–O bond length does not practically change [2.14 Å (300 K) ÷ 2.15 Å (7 K)] (see Table 1). It differs from the results of [10], where an increase of both the Bi–O bond lengths by 0.03 Å at low temperature was observed. It was postulated [10] that the increase of Bi–O bond lengths may be a result of the structural phase transformation from the monoclinic I2/m to monoclinic P2/m structure observed by Pei et al. [7] at ~ 140 K. But Thornton and Jacobson [12] in a neutron diffraction study found the same structure of $BaBiO_3$ at 293 and 4.2 K with slightly larger atom displacements from the ideal positions at the lower temperature. Pei et al. [7] assumed that this discrepancy originates from some sample dependent variables (such as the oxygen content), which was not accurately characterized. In addition, Koyama et al. [15] (electron diffraction) did not find any phase transition in $BaBiO_3$ down to 100 K.

The most important peculiarity of our results is an abnormal temperature dependence of the Bi–O bond Debye–Waller factors for compounds with $x = 1.0$ and 0.75 at temperature range 7 ÷ 90 K. As can be seen from Fig. 3 and Table 1, the DW-factors of

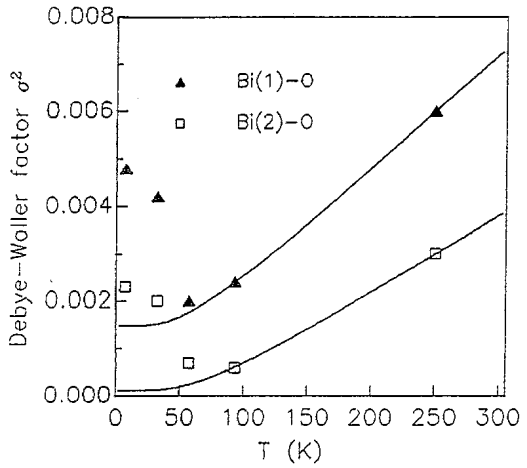

Fig. 3. Temperature dependent σ^2 of oxygen shells in $BaBiO_3$ with the longer bond length (▲) and with the shorter bond length (□). The solid lines are the Einstein model fits.

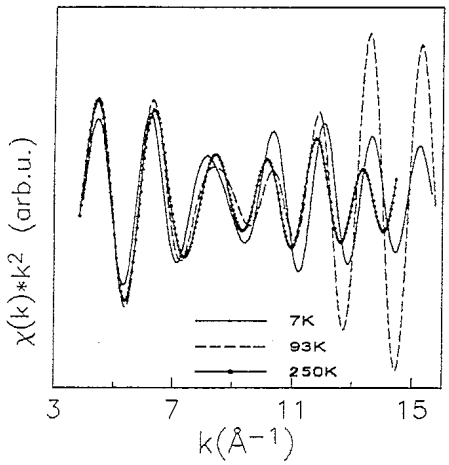

Fig. 4. First (oxygen) shell from Bi L_3 edge for $BaBiO_3$ at different temperatures: 7, 90 and 250 K.

both Bi–O bonds appear to increase with the decreasing temperature. In addition, σ^2 of the longer Bi–O bond shows a stronger temperature dependence than that of the shorter bond. Heald et al. [9] also performed similar experiments for a BaKBiO system and found for $x = 0.4$ a small deviation of σ^2 from the harmonic extrapolation. For the pure $BaBiO_3$ they obtained two different $\sigma^2(T)$ dependencies for the two Bi–O bonds which demonstrates a strong difference between the two Bi sites. The approximation of $\sigma^2(T)$ dependencies according to the Einstein model showed two different Einstein temperatures for the two Bi–O bonds. At the same time, the authors pointed out some scattering of experimental points at low temperatures. Comparing our results with those of Ref. [9], we suppose that in this scattering one can see a tendency of the increase of σ^2 at low temperatures. A similar tendency can be seen in Ref. [10]. From the Einstein model's point of view, which should fit well with the temperature dependence of harmonic systems, this tendency is absolutely abnormal.

To illustrate the reality of our results, the isolated first shell of $k^2 * \chi(k)$ for $BaBiO_3$ at three temperatures (7, 93 and 250 K) is presented in Fig. 4. One can see that the beating at 93 K is stronger not only than the beating at 250 K but also than the beating at 7 K, which indicates that at 93 K the contributions of the two Bi–O shells are almost equal, so that their

interference in the EXAFS spectra has a maximum effect near this temperature. In the case of the ordinary $\sigma^2(T)$ dependence for the two Bi–O bonds the strongest beat would be observed at the lowest temperature.

Some differences between our results and earlier EXAFS studies [9–11] seem to arise from the different window width at the back Fourier transform operations. We now used a wider window 1.1 Å compared with 0.7 Å ([11], for Pb–O sphere) for the BFT, choosing it at the points where the imaginary part of the FT function becomes zero. The shortening of the window width leads to a partial loss of real information about the first oxygen shell.

5. Discussion

The increase of the Bi–O, Bi(Pb)–Ba bond lengths and abnormal $\sigma^2(T)$ behaviour in pure and slightly Pb doped $BaBiO_3$ can be explained by taking into account the nature of the lattice distortions in the perovskite structure.

It is known [4,5] that the monoclinic distortion of $BaBiO_3$ cubic lattice arises from a rigid tilt of oxygen octahedra around the pseudocubic [110] axes accompanied by the breathing mode distortion. The static tilt angle ϕ of the oxygen octahedra appears to increase with the temperature decrease [4,5,7], which should lead to the increasing Bi–O bond length observed by Salem-Sugui et al. [10] and in the current study (see Table 1). As was pointed out, we have obtained an increase only for the longer Bi–O bond length, while the shorter one practically does not change. It coincides with a different behaviour of two Bi–O distances found by Heald et al. [9] and in the current study as the different temperature dependencies of the DW-factors (see Fig. 3). The shorter bond has a higher characteristic temperature (490 K [9]) than the longer one and is stiff, while the longer bond (340 K [9]) is soft [11]. This result is in full agreement with our conclusion from XANES study of the Bi valence state [16]. We showed that bismuth in $BaBiO_3$ is situated in two different positions with Bi^{3+} and $Bi^{3+}\underline{L}^2$ valence states, where $\underline{L}^2$ denotes the presence of two holes in the nearest oxygen environment. It causes a difference in the two Bi–O bond strengths. That is why the stiff octahedra with shorter Bi–O bonds, containing a hole pair do practically not change their radii. At the same time the radii of octahedra with soft longer Bi–O bonds have a tendency to increase with the growing tilting distortion. Thus, there is an essential asymmetry in the static rotation of the oxygen octahedra: the small octahedron rotates with an almost constant short Bi–O bond length R_s, while the large octahedron shows an increase of the long Bi–O bond length R_l with the tilting angle increasing. It leads to the growth of the difference between the two bond lengths Δr from 0.15 Å (250 K) to 0.19 Å (7 K) (Table 1). In other words, the changes of the tilting distortion produce the additional changes of the breathing mode distortion due to the difference in the Bi–O bond strengths. Similar behaviour of the Bi–O bond lengths was also observed for slightly doped $BaPb_{0.75}Bi_{0.25}O_3$ (Table 1). It is worth noticing that the dependence of Bi–O bonds behaviour on K contents in BKB compounds [9,10] confirms our conclusions. Indeed, with the K contents increasing from 0 to 0.37, the static tilting angle ϕ of oxygen octahedra decreases from $\sim 10°$ [7] to zero. As a result, both Bi–O bond lengths become equal and close in their values to the shorter one in $BaBiO_3$. Besides, the temperature dependence of the DW-factor of the Bi–O bond in cubic $Ba_{0.6}K_{0.4}BiO_3$ practically coincides with the temperature dependence of the DW-factor of the shorter bond in $BaBiO_3$. Thus, due to the asymmetry of the Bi–O bonds the disappearance of the static tilting distortion with K-doping leads to the disappearance of breathing distortion.

The rotation asymmetry of two different Bi–O bonds becomes more pronounced in the temperature dependencies of dynamic fluctuations of both tilting and breathing modes. It is well known that the vibration of oxygen atoms has a strong anisotropy for $BaBiO_3$ [5] as well as for both BPB and BKB compounds [6–8]. For example, in $Ba_{0.87}K_{0.13}BiO_3$ [6] the oxygen displacements perpendicular to the Bi–Bi direction due to the tilting mode fluctuation of the oxygen octahedra more than two times, overcome the displacements of the breathing mode in the parallel direction. In addition, Cox and Sleigtht [5] pointed to a strong asymmetry of the $BaBiO_3$ oxygen atom thermal vibration matrix with large off-diagonal terms, which coincides with our conclusion

that the two Bi–O bonds have a noticeable asymmetry of the tilting distortion.

The tilting vibration displacement is perpendicular to the Bi–O direction and such a motion would not contribute strongly to the EXAFS DW-factor σ^2, which is sensitive only to changes in the Bi–O bond length [9]. Meanwhile, the rotation asymmetry of the two octahedra produces the changes in Bi–O lengths due to the change of the tilting angle. As a result, the dynamic fluctuation of the tilting mode will lead to additional fluctuations of the Bi–O bond lengths. Thus, the values of the Debye–Waller factor σ^2 of Bi–O bonds extracted from the EXAFS spectra should contain at least two parts: σ_b^2 and σ_t^2 from the breathing and tilting modes respectively. At high temperatures ($T > 90$ K) the value of σ_t^2 is negligible in comparison with σ_b^2 and the temperature dependencies of the DW-factor σ^2 are in the agreement with the Einstein model.

With decreasing temperature, the static tilting angle grows [4,7], which increases both the long Bi–O distance and the contribution from the tilting fluctuations into σ^2 value. Koyama and coworkers [15,17] concluded from the electron diffraction measurements that the fluctuation of the tilting displacement becomes remarkable on cooling due to the softening of the rotation phonon mode. Thus, the anomalous increase of the DW-factors at the temperature fall for monoclinic distorted $BaBiO_3$ arises from the σ_t^2 contribution to the $\sigma^2(T)$ temperature dependence (see Fig. 3).

Apparently, due to the essential difference in the Bi–O bond strengths, the fluctuation asymmetry of the tilting mode is considerable and it leads to a negative thermal expansion coefficient [14]. It was observed as the Bi–Ba bond length growth for both the $BaBiO_3$ and $BaPb_{0.25}Bi_{0.75}O_3$ compounds in our experiments (see Table 1).

The other BPB end member, $BaPbO_3$, has a weak lattice distortion in contrast to monoclinic distortions of $BaBiO_3$. All Pb–O bonds have the same strength. The oxygen octahedra around the Pb atoms are equivalent. That is why the Pb–O bond length and its DW-factor show an ordinary growth with temperature, unlike those in $BaBiO_3$ and $BaPb_{0.75}Bi_{0.25}O_3$.

In the superconducting BPB compound with $x = 0.25$ our previous results also showed an ordinary increase of Bi–O and Bi–Ba bond lengths with temperature. Probably it is connected with a less distorted structure compared with $BaBiO_3$ due to a small bismuth content [4]. Nevertheless, it would be very interesting to obtain the $\sigma^2(T)$ dependence of the Bi–O bonds since it could help to explain the coexistence of the breathing mode distortion and superconductivity in this compound.

As pointed out by Heald et al. [9], a tendency towards the rotational distortion may also remain in the cubic BKB ($x = 0.4$) material. This tendency would be expected to modify the temperature dependence of Bi–O σ^2 and to produce deviations from the harmonic behaviour.

Thus, using the dynamic fluctuation tilting mode model, it is possible to explain practically all the local structure anomalies, observed in this work and in Refs. [9,10]. At the same time, from the EXAFS experiments we can not exactly affirm whether dynamic fluctuations or randomly distributed structural disorder would be consistent with the above results. EXAFS study should be accompanied by additional diffraction (neutron, X-ray and electron) measurements.

A possible connection of the tilting mode fluctuation with superconductivity in BKB, BPB systems was noticed in a number of studies [15,17,18]. The rotation type vibration mode of oxygen octahedra plays the main role in the anharmonic model for high-T_c superconductors by Plakida et al. [19]. That is why it is necessary to carry out more accurate investigations of low temperature features of the local structure in the superconducting phases BaPbBiO ($0 < x < 0.35$) and BaKBiO ($0.37 < x < 0.5$). Such a study is under way (see preliminary results in Ref. [20]) and will be published later.

6. Conclusion

Our low temperature EXAFS-study revealed essential anomalies of the $BaBiO_3$ and $BaPb_{0.75}Bi_{0.25}O_3$ local structure. These anomalies are connected with peculiarities of the distorted perovskite lattice structure at low temperatures. We have shown that presence of two different Bi positions in $BaBiO_3$ arising from the difference in the bond strengths leads to essential asymmetry of the tilting distortion. The asymmetry produces an abnor-

mal behaviour of the Bi–O bond lengths at low temperature: the longer bond length essentially increases, while the shorter does in fact not change. The dynamic fluctuation of the tilting mode causes an abnormal increase of the Bi–O bond DW-factors for $BaBiO_3$ and $BaPb_{0.75}Bi_{0.25}O_3$ with decreasing temperature. The deviation of Bi–O bond $\sigma^2(T)$ from the Einstein model was observed for cubic BKB with $x = 0.4$ [9].

The other BPB end member $BaPbO_3$ has equivalent Pb positions and is characterized by the symmetric tilting mode fluctuation of the Pb–O bond. The temperature dependencies of Pb–O bond length and its DW-factor show an ordinary growth with temperature.

Acknowledgements

The authors (excluding S.B.) are very grateful to Prof. H. Dexpert and the LURE program committee for supporting our projects PS-207 and PS-056 at LURE. This work was supported by grant MG-2300 of International Science Foundation and Russian Government by grant 96-02-19099a of RFBR and the State program 'Universities of Russia'.

References

[1] A.W. Sleight, J.L. Gillson, P.E. Bierstedt, Solid State Commun. 17 (1975) 27.
[2] J.G. Bednorz, K.A. Muller, Z. Phys. B 64 (1986) 189.
[3] M. Shirai, N. Suzuki, K. Motizuki, J. Phys. Condens. Matter 2 (1990) 3553.
[4] D.T. Marx, P.G. Radaelli, J.D. Jorgensen, R.L. Hitterman, D.G. Hinks, S. Pei, B. Dabrowski, Phys. Rev. B 46 (1992) 1144.
[5] D.E. Cox, A.W. Sleight, Acta Crystallogr. B 35 (1979) 16.
[6] J.P. Wignacourt, J.S. Swinnea, H. Steinfink, J.B. Goodenough, Appl. Phys. Lett. 53 (1988) 1753.
[7] S. Pei, J.D. Jorgensen, B. Dabrowski, D.G. Hinks, D.R. Richards, A.W. Mitchell, J.M. Newsam, S.K. Sinha, D. Vaknin, A.J. Jacobson, Phys. Rev. B 41 (1990) 4126.
[8] G.H. Kwei, J.A. Goldstone, A.C. Lawson Jr., J.D. Thompson, A. Williams, Phys. Rev. B 39 (1988) 7378.
[9] S.M. Heald, D. DiMarzio, M. Croft, M.S. Hegde, S. Li, M. Freenblatt, Phys. Rev. B 40 (1989) 8828.
[10] S. Salem-Sugui Jr., E.E. Alp, S.M. Mini, M. Ramanathan, J.C. Campuzano, G. Jennings, M. Faiz, S. Pei, B. Dabrovski, Y. Zheng, D.R. Richards, D.G. Hinks, Phys. Rev. B 43 (1991) 5511.
[11] J.B. Boyce, F.G. Bridges, T. Claeson, T.H. Geballe, G.G. Li, A.W. Sleight, Phys. Rev. B 44 (1991) 6961.
[12] G. Thornton, A.J. Jacobson, Acta Crystallogr. B 34 (1978) 351.
[13] C. Chaillout, A. Santoro, J.P. Remeika, A.S. Cooper, G.P. Espinosa, Solid State Commun. 65 (1988) 363.
[14] N.V. Anshukova, A.I. Golovashkin, Yu.V. Bugoslavskii, L.I. Ivanova, A.P. Rusakov, I.B. Krinetskii, J. Supercond. 7 (1994) 427.
[15] Y. Koyama, M. Ishimaru, Phys. Rev. B 45 (1992) 9966.
[16] A.Yu. Ignatov, A.P. Menushenkov, K.V. Klementev, D.I. Kochubey, Nucl. Instrum. Meth. Phys. Res. A 359 (1995) 244.
[17] Y. Koyama, S.-I. Nakamura, Y. Inoue, Phys. Rev. B 46 (1992) 9186.
[18] A.I. Liechtenstein, I.I. Mazin, C.O. Rodriguez, O. Jepsen, O.K. Andersen, M. Methfessel, Phys. Rev. B 44 (1991) 5388.
[19] N.M. Plakida, V.L. Aksenov, S.L. Drechsler, Proceedings of the Adriatico Research Conference on HTSC, Trieste, World Scientific, Singapore, 1987, p. 1071.
[20] A.P. Menushenkov, S. Benazeth, J. Purans, A.Yu. Ignatov, K.V. Klementev, Abstracts of IV International Workshop on Chemistry and Technology of HTSC, Moscow, 1995, p. 70.